

## Pair potentials for fcc metals

M. I. Baskes and C. F. Melius  
*Sandia Laboratories, Livermore, California 94550*  
 (Received 19 April 1979)

Long-range pair potentials are presented for the fcc metals Ni, Au, Ag, Pt, Pd, Cu, and Al. Experimental data considered in deriving the potentials include the sublimation energies and stacking-fault energies as well as the lattice parameters, elastic constants, and vacancy-formation and -migration energies. A volume-dependent energy term has been included in the potentials. By scaling the potentials with respect to lattice spacing and a characteristic binding energy, a striking similarity can be seen between the various potentials. These potentials have been used to calculate a variety of point-defect properties including self-interstitial geometries and migration energies. In addition the migration energy of helium and its binding energy to a vacancy have been calculated.

### I. INTRODUCTION

Problems such as radiation damage in solids (e.g., impurities and implanted atomic species interacting with vacancies, self-interstitials, and dislocations) have been treated in the past using the lattice-defect method.<sup>1</sup> The treatment of extended defects in fcc metals (e.g., dislocations) requires pair potentials which include stacking-fault energies. A large number of diverse pair potentials have been proposed in the literature for use in various fcc metals.<sup>1-5</sup> The major purpose of this paper is to derive new pair potentials for a number of fcc materials which are consistent with experimental data (including stacking-fault energies as well as sublimation energies) and which also properly take into account the volume-dependent energy term.

In Sec. II the pair-potential formalism is presented, while in Sec. III the calculation of the potentials is presented. A discussion of these potentials and a comparison with previously published potentials appears in Sec. IV. Also in Sec. IV, the new potentials are used to calculate a number of simple point-defect properties. Conclusions are presented in Sec. V.

### II. THEORY

Various methods for obtaining pair potentials and their subsequent use in point-defect calculations have recently been reviewed by Johnson.<sup>1</sup> In general it is assumed<sup>6</sup> that the energy  $E$  of a monatomic crystal per unit undeformed volume may be expressed as a sum of two terms

$$E = N_A E_b + N_L E_v, \quad (1)$$

where  $E_b$  is the bond energy per atom,  $N_A$  is the number of atoms,  $E_v$  is a volume-dependent energy per undeformed lattice site, and  $N_L$  is the number of

undeformed lattice sites. The bond energy is given by a simple sum over all other atoms

$$E_b = \left(\frac{1}{2}\right) \sum_m \phi(\bar{r}_m), \quad (2)$$

where  $\phi(\bar{r}_m)$  is the pair potential between two atoms separated by a distance  $\bar{r}_m$ . A general form for the volume-dependent term has previously been proposed<sup>7</sup>

$$E_v = \Omega_0 \sum_q P_q (V/V_0)^q, \quad (3)$$

where  $\Omega_0$  is the undeformed atomic volume, the  $P_q$  are constants,  $V$  is the deformed volume, and  $V_0$  is the undeformed volume. In this work a more specific volume-dependent term is used, i.e.,

$$E_v = \Omega_0 (V/V_0) [p_0 + \frac{1}{2} p_2 (\Delta V/V_0)^2], \quad (4)$$

where  $\Delta V = V - V_0$  is the volume change due to deformation and  $p_0$  and  $p_2$  are constants. A complete discussion of the volume-dependent term is found in Appendix A.

Using the previously derived equations for a central potential in an fcc material,<sup>7</sup> the following expressions for the elastic constants  $C_{11}$ ,  $C_{12}$ , and  $C_{44}$  are obtained

$$\begin{aligned} C_{11} &= B_{11} - p_0 + p_2, \\ C_{12} &= B_{12} + p_0 + p_2, \\ C_{44} &= B_{12} - p_0, \end{aligned} \quad (5)$$

where

$$\begin{aligned} B_{11} &= \frac{1}{2\Omega_0} \sum_m \left[ \frac{1}{a^m} \right]^2 \left( \phi_m'' - \frac{\phi_m'}{a^m} \right) (a_1^m)^4, \\ B_{12} &= \frac{1}{2\Omega_0} \sum_m \left[ \frac{1}{a^m} \right]^2 \left( \phi_m'' - \frac{\phi_m'}{a^m} \right) (a_1^m)^2 (a_2^m)^2. \end{aligned} \quad (6)$$

The summation is over all atoms a distance  $a^m$  from the origin,  $a_1^m$  and  $a_2^m$  are the projections of this distance in the directions defined by 1 and 2, and  $\phi_m'$  and  $\phi_m''$  are the appropriate first and second derivatives of the potential at this distance. In addition, equilibrium requires<sup>7</sup> that

$$p_0 = -\frac{1}{2\Omega_0} \sum_m \left( \frac{\phi_m'}{a^m} \right) (a_1^m)^2. \quad (7)$$

Using the above formalism, it is possible to obtain expressions for additional experimental quantities. The vacancy-formation energy  $E_{fV}^f$ , i.e., the energy required to move an atom from inside the lattice to the surface (keeping the total number of lattice atoms fixed), is given by

$$E_{fV}^f = -E_b + p_0\Omega_0 - \Delta E_{fV}^f. \quad (8)$$

The first term represents the bond energy required to form the vacancy by removing an atom from an internal lattice site and placing that atom at a newly created lattice site on the surface. The second term arises from the increase in the number of lattice sites by one required by this process, while the third term represents the reduction in energy due to lattice relaxations. The small change in volume due to lattice relaxation contributes an additional small volume-dependent energy correction to this third term which has been neglected.

In similar fashion, the sublimation energy  $E_s$ , i.e., the energy required to remove a surface atom to infinity (leaving no vacancies or surface rearrangement), is given by

$$E_s = -E_b - p_0\Omega_0. \quad (9)$$

As in Eq. (8), the first term represents the change in bond energy and the second results from the required volume change. Note that no lattice relaxation term exists in Eq. (9) since there are no lattice defects created by this process.

The energy required to remove a bulk atom to infinity  $E_0$  (leaving a vacancy in the lattice) is simply the sum of the vacancy-formation energy and the sublimation energy

$$E_0 = E_{fV}^f + E_s = -2E_b - \Delta E_{fV}^f. \quad (10)$$

While this quantity is not directly observable by experiment it plays an important theoretical role in the scaling relationships discussed in Sec. III.

The stacking-fault energy  $\gamma$  can be calculated by simple bond counting at the (111) interface between a fcc and hcp material, and is given by

$$\gamma = \left\{ \left[ 2\phi \left( \frac{2b}{\sqrt{3}} \right) \right] - 6\phi \left( \sqrt{\frac{3}{2}}b \right) + 12\phi \left( \sqrt{\frac{11}{6}}b \right) \right\} \frac{12^{1/2}b}{6\Omega_0}, \quad (11)$$

where  $b$  is the lattice constant. This expression assumes a potential interaction range of less than fourth neighbors ( $\sqrt{2}$  lattice constants).

Using these relationships [Eqs. (1)–(11)], one can obtain a two-body metal-metal potential fit to the corresponding experimental data. The procedure is discussed in Sec. III.

### III. CALCULATION OF THE PAIR POTENTIALS

The basic method used to calculate the pair potentials involves (i) the selection of a functional form (with a number of free parameters) for the potential, and (ii) the variation of the parameters so that the various calculated quantities agree (in a least-squares sense) with the corresponding experimental data. The functional form used here is simply a cubic spline between a number of fixed-node points. This form assures continuity of the potential and its first two derivatives. The free parameters are the values of the pair potential at the node points. Since the potential is to be used in lattice-defect calculations, a smooth, finite range potential is required. The distance  $r_c$  at which the potential goes smoothly to zero is a free parameter. Since stacking-fault energies are to be included in the potential fit,  $r_c$  must extend to at least third nearest neighbors. An important additional constraint which has been imposed upon the parameters is that the pair potential be as smooth as possible (in a semiquantitative sense); that is, that the number of changes in sign of the derivatives of the potential (or "wiggles") must be kept to a minimum, and no arbitrary barriers (or humps) should occur in the potential-energy curve. This constraint avoids the creation of spurious minima in the lattice-defect calculations.

The experimental data that is used in the fitting procedure is shown in Table I. Consistent values of the lattice parameter  $b$ ,<sup>8</sup> the elastic constants  $C_{11}$ ,  $C_{12}$ , and  $C_{44}$ ,<sup>9</sup> and the sublimation energy  $E_s$ ,<sup>10</sup> are easily found in the literature. On the contrary, values of the vacancy-formation energy  $E_{fV}^f$  and -migration energy  $E_{fV}^M$  are not easily measured and considerable variation in these values may be found in the literature.<sup>11</sup> Reasonable estimates of the available data are used knowing full well that controversy resulting from these choices may result. A similar situation exists for stacking-fault energy data  $\gamma$ . Again, reasonable estimates are made from the many values found in the literature.<sup>12</sup> In the past the experimental phonon-dispersion curves have been used to determine potentials. Since the elastic constants are simply the long-wavelength limit of the data, the dominant aspects of the phonon dispersion curves are already incorporated into the pair potentials through the fitting of the elastic constants.

None of the data considered thus far concerns the

TABLE I. Quantities used for the determination of the potentials. The lattice parameter  $b$ , the elastic constants,  $C_{11}$ ,  $C_{12}$ , and  $C_{44}$ , the sublimation energy  $E_s$ , the vacancy-formation and -migration energies  $E_{fV}^F$  and  $E_{mV}^M$ , the surface energy  $\gamma$ , the free-electron potential slope  $\alpha$ , and the scaling parameter  $E_0 = E_s + E_{fV}^F$  are given for each of the fcc metals.

	Ni	Au	Ag	Pt	Pd	Cu	Al
$b$ (Å) <sup>a</sup>	3.52	4.07	4.08	3.92	3.89	3.62	4.05
$C_{11}$ ( $10^{12}$ dynes/cm <sup>2</sup> ) <sup>b</sup>	2.465	1.86	1.240	3.467	2.341	1.700	1.12
$C_{12}$ ( $10^{12}$ dynes/cm <sup>2</sup> ) <sup>b</sup>	1.473	1.57	0.934	2.507	1.761	1.225	0.66
$C_{44}$ ( $10^{12}$ dynes/cm <sup>2</sup> ) <sup>b</sup>	1.247	0.42	0.461	0.765	0.712	0.758	0.279
$E_s$ (eV) <sup>c</sup>	4.45	3.93	2.85	5.77	3.91	3.54	3.58
$E_{fV}^F$ (eV) <sup>d</sup>	1.4	1.0	1.1	1.5	1.4	1.15	0.75
$E_{mV}^M$ (eV) <sup>d</sup>	1.4	0.85	0.8	1.35	1.3	0.9	0.7
$\gamma$ (ergs/cm <sup>2</sup> ) <sup>e</sup>	125	55	20	110	100	73	160
$\alpha$ (eV/Å)	-3.62	-5.45	-2.96	-5.92	-5.0	-2.34	-3.0
$E_0$ (eV)	5.85	4.93	3.95	7.27	5.31	4.69	4.31

<sup>a</sup>Reference 4.

<sup>b</sup>Reference 5.

<sup>c</sup>Reference 6.

<sup>d</sup>Reference 7.

<sup>e</sup>Reference 8.

behavior of the potential at distances less than the nearest-neighbor (0.707 lattice spacings) distance, yet such information is needed to determine the formation and migration energy of self-interstitials, whose interactions involve distances from 0.6 to 0.7 lattice spacings. Therefore free-electron two-body interactions<sup>2</sup> have been used to help determine the potential at short range. Specifically the slope of the potential (at a distance of 0.60 lattice spacings) is constrained to equal that obtained in a free-electron calculation. The slopes  $\alpha$ , are included in Table I. The slope, rather than the function itself, is used since it has been shown previously<sup>13</sup> that while free-electron calculations (ignoring the conduction electrons) have an undetermined zero shift in the energy, the slope agrees well with a complete quantum-mechanical calculation. For each of the transition-metal atoms, an

atomic core (corresponding to a charge state of +1) was used for the free-electron calculation. For aluminum (a nontransition metal) it is not obvious what core to use. Our calculations using Al<sup>3+</sup>, Al<sup>+</sup>, and Al<sup>0</sup> states yielded calculated self-interstitial configurations which were in disagreement with experiment. To obtain agreement with the experimental data  $\alpha$  has been chosen to be -3.0 eV/Å, which is a larger value than those calculated for any of the above charge states. As is shown below, the use of this value of  $\alpha$  results in an Al pair potential quite similar in shape to the transition-metal pair potentials.

Atomic relaxations are considered when calculating the vacancy-formation and -migration energies. In addition, it is shown in Appendix B that the volume-dependent energy term  $E_v$  [see Eq. (3)] introduces a minor (<0.001 eV) change in the vacancy-formation

TABLE II. Parameters used to define the potentials. The coefficients in the volume-dependent energy term,  $p_0$  and  $p_2$ , the potential values at the spline knots  $\phi$ , the cutoff distance  $r_c$ , and the slope of the potential at this distance  $\phi'(r_c)$  are given for each of the fcc metals.

	Ni	Au	Ag	Pt	Pd	Cu	Al
$p_0$ <sup>a</sup>	-0.1394	-0.0870	-0.0523	-0.1418	-0.0856	-0.1003	-0.0846
$p_2$ <sup>a</sup>	0.4202	0.8983	0.4015	1.3725	0.8401	0.4926	0.4073
$\phi(0.6b)$ <sup>b</sup>	0.0504	0.2793	0.0660	0.5443	0.1416	0.0444	0.1271
$\phi(0.7b)$ <sup>b</sup>	-0.4138	-0.3534	-0.2858	-0.4944	-0.3879	-0.3285	-0.2548
$\phi(0.8b)$ <sup>b</sup>	-0.3078	-0.2738	-0.2195	-0.3979	-0.2901	-0.2614	-0.2350
$\phi(0.9b)$ <sup>b</sup>	-0.1415	-0.1478	-0.1181	-0.2257	-0.1290	-0.1397	-0.1301
$\phi(1.0b)$ <sup>b</sup>	-0.0715	-0.0733	-0.0592	-0.1307	-0.0563	-0.0709	-0.0882
$\phi(1.1b)$ <sup>b</sup>	-0.0455	-0.0334	-0.0269	-0.0639	-0.0278	-0.0371	-0.0636
$\phi(1.2b)$ <sup>b</sup>	-0.0245	-0.0141	-0.0091	-0.0295	-0.0160	-0.0175	-0.0367
$r_c$ <sup>c</sup>	4.841	5.511	5.524	5.407	5.270	4.988	5.548
$\phi(r_c)$ <sup>b</sup>	0.0	0.0	0.0	0.0	0.0	0.0	0.0
$\phi'(0.6b)$ <sup>d</sup>	-3.620	-5.463	-2.684	-5.921	-4.516	-2.340	-3.000
$\phi'(r_c)$ <sup>d</sup>	0.0	0.0742	0.0285	0.0	0.1494	0.0	0.0

<sup>a</sup>Units are eV/Å<sup>3</sup>.

<sup>b</sup>Units are eV.

<sup>c</sup>Units are Å.

<sup>d</sup>Units are eV/Å.

and -migration energies. Thus, no large correction due to  $E_v$  should be included explicitly in fitting to  $E_{fV}^f$ , as has erroneously been done by others.<sup>3</sup>

The resulting parameters for each of the potentials are given in Table II. It should be noted that the potential is completely determined by the eight function values plus the two slopes at the end points given in Table II. In all cases, the experimental data have been fitted to better than their estimated uncertainty. All elastic constants are fit to <1.2%, sublimation energies to <0.4%, vacancy-formation and -migration energies to <5%, stacking-fault energies to <15%, and free-electron slopes to <10%. The resulting contribution of the volume-dependent terms to the elastic constants [Eq. (5)] has been found to be quite significant. For instance over 80% of the bulk modulus for Au comes from the volume-dependent terms. This large contribution is perhaps indicative of problems that have been encountered in the fitting and use of Au pair potentials.<sup>1</sup>

#### IV. DISCUSSION OF THE POTENTIALS AND APPLICATIONS

##### A. Potentials

A comparison of the Ni and Cu potentials derived in Sec. III with a number of potentials from the literature<sup>2-5</sup> is given in Fig. 1. Qualitatively, the potentials are all similar. Note, however, that while the previous long-range potentials include an oscillation to fit the stacking-fault energy, the current potentials have not only fit more data than the older long-range potentials, but have done so without the need for a long-range repulsive barrier.

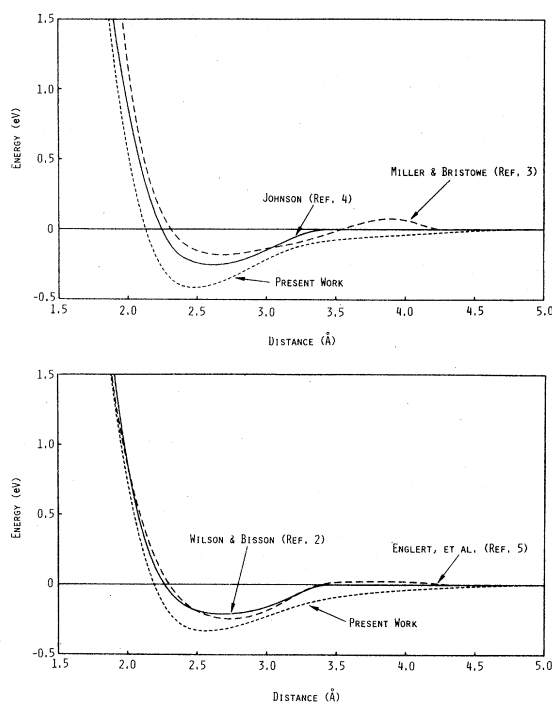


FIG. 1. Comparison of nickel (a) and copper (b) pair potentials to short-range and long-range potentials from the literature.

An attempt has been made to compare the seven fcc potentials with each other. In order to effect a meaningful comparison, two scaling parameters are used, the lattice parameter and  $E_0$ , the energy required to remove an atom from the lattice. Numerical values of these scaling parameters may be found in Table I. The scaled curves (Fig. 2) have a striking

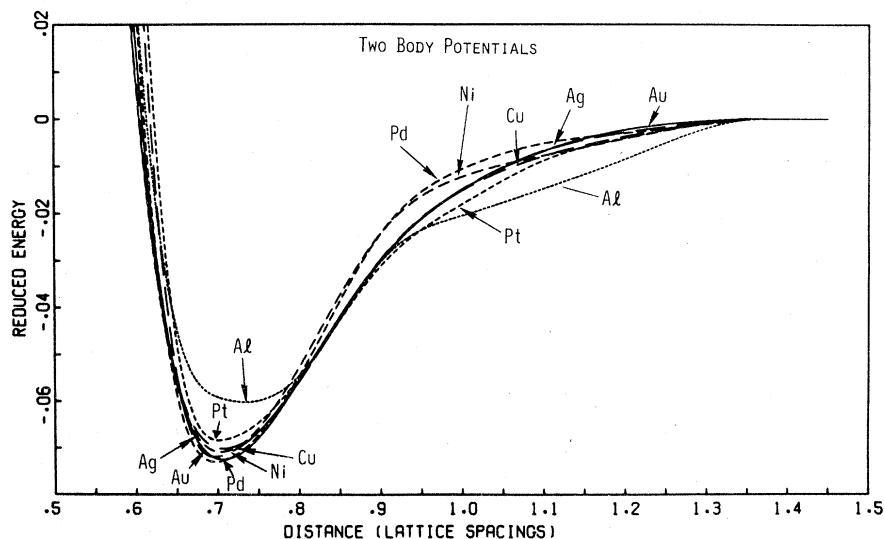


FIG. 2. Scaled pair potentials for fcc metals. The energy is scaled by the sum of the sublimation energy and vacancy formation energy.

similarity with the scaled minima all having about the same magnitude and scaled position. This minimum position occurs at about the first-neighbor position ( $\frac{1}{2}\sqrt{2}$  lattice spacings). The pair potential for Al (the only nontransition element considered here) differs somewhat from the other potentials. Part of the difference, particularly at long range, can be attributed to the relatively large stacking-fault energy found for Al. Changing the slope  $\alpha$  (discussed in Sec. III) does not significantly affect the shape of the potential beyond the nearest-neighbor distance.

### B. Point defects

In order to further compare the new potentials with previous results, a number of point-defect calculations have been performed. The general procedure used for these calculations is the lattice-defect method.<sup>1</sup> A spherical movable region of  $\sim 680$  atoms with fixed boundary atoms has been used. A complete discussion of the effect of volume changes is given in Appendix B where it is shown that a fixed boundary calculation is able to give an accurate energy. The relaxed energy for a vacancy needed in Sec. III has been calculated in the same manner discussed here. The helium-metal pair potentials (except for Ni) are obtained from a free-electron calculation and are shown in Fig. 3. The He-Ni potential is obtained from a more exact nickel cluster calculation.<sup>13</sup> Due to the inclusion of electronic effects this more realistic He-Ni potential is "softer" than the free-electron potentials. Note that the He-Al potential (Al being a nontransition metal) differs considerably from the transition-metal potentials.

The results for a large number of point-defect calculations are summarized in Table III. As with the

experimental vacancy-formation and -migration energy data used in determining the pair potentials, considerable variation and interpretation of the experimental data in Table III exists in the literature.

While reasonable estimates of the available data are given it is to be emphasized that differences between theoretical and experimental values may be due to experimental uncertainty or interpretation as well as to limitations of the pair potentials. Overall agreement between theory and experiments is quite satisfying, with differences of several tenths of an eV being within the accuracy of the pair potential model.

The self-interstitial formation energy  $E_{f_i}^I$  ranges from a high of 6.42 eV for Pt to a low of 2.50 eV for Al, while the interstitial migration energy  $E_{1_i}^M$  is small ( $< 0.25$  eV) in all cases. Formation energies are not experimentally accessible, but the low values of the migration energy are in agreement with the experimental measurements and current models of low-temperature resistivity recovery.<sup>14</sup> The orientation of the split interstitial is calculated to be along the  $\langle 100 \rangle$  direction for all of the fcc metals considered. Experimental measurements of interstitial orientation have been made for Cu,<sup>15</sup> and Al,<sup>16</sup> and are in agreement with the calculated direction. Calculated values of the anisotropy of the interstitial dipole tensor  $P_{11} - P_{12}$  using the method of Hardy<sup>17</sup> are also given in Table III. Agreement is within the experimental error for Al ( $1.1 \pm 0.3$  eV).<sup>16</sup> Frenkel-pair formation energies  $E_{FP}$  have been calculated to lie in the range of 7.90 eV for Pt to 3.21 eV for Al. Reliable experimental Frenkel-pair formation energies have not been found for comparison.

First-neighbor divacancy binding energies  $E_{2V}^B$  are calculated to be about the strength of one first-neighbor bond. Agreement with the experimental

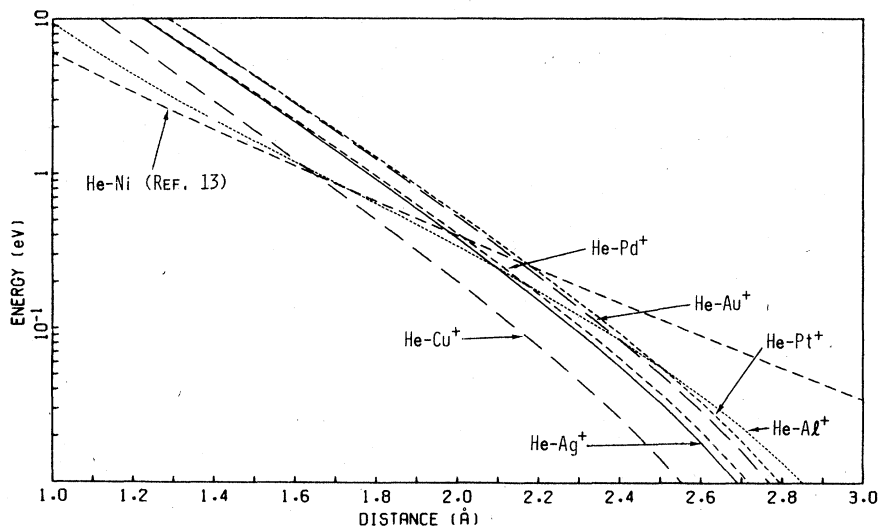


FIG. 3. Free-electron helium-metal pair potentials.

TABLE III. Calculated point-defect energies.<sup>a</sup> The self-interstitial formation energy, anisotropy, and migration energy,  $E_{II}^F$ ,  $P_{11} - P_{12}$ , and  $E_{II}^M$ , Frenkel-pair formation energy  $E_{FP}$ , divacancy binding and migration energy,  $E_{2V}^B$  and  $E_{2V}^M$ , and helium formation, migration, and binding energy to a vacancy,  $E_{He}^F$ ,  $E_{He}^M$ , and  $E_{HeV}^B$  are given for each of the fcc metals.

	Ni	Au	Ag	Pt	Pd	Cu	Al
$E_{II}^F$	4.90	3.70	3.11	6.42	4.93	3.46	2.50
$P_{11} - P_{12}$	5.15	2.93	4.11	2.72	4.69	3.54	0.88 (1.1 ± 0.3) <sup>b</sup>
$E_{II}^M$	0.24 (0.15) <sup>c</sup>	0.08	0.13	0.15 (0.06) <sup>c</sup>	0.19	0.13 (0.12) <sup>c</sup>	0.07 (0.12) <sup>c</sup>
$E_{FP}$	6.31	4.68	4.21	7.90	6.34	4.61	3.21
$E_{2V}^B$	0.44 (0.33) <sup>d</sup>	0.43 (0.1) <sup>e</sup>	0.30 (0.38) <sup>f</sup>	0.55 (0.40) <sup>f</sup>	0.40	0.35 (0.12) <sup>g</sup>	0.28 (0.25) <sup>g</sup>
$E_{2V}^M$	1.17 (0.83) <sup>d</sup>	0.78 (0.71) <sup>f</sup>	0.61 (0.57) <sup>f</sup>	1.06 (1.1) <sup>f</sup>	1.05	0.72 (0.71) <sup>f</sup>	0.45 (0.42) <sup>f</sup>
$E_{He}^F$	4.02	1.60	1.32	2.60	2.18	1.93	1.32
$E_{He}^M$	0.66	0.72	0.65	1.13	0.94	0.63	0.33
$E_{HeV}^B$	2.63 (2.1) <sup>h</sup>	1.58	1.32	2.48	2.10	2.13	1.22 (1.0) <sup>i</sup>

<sup>a</sup>Units are eV. Experimental values in ( ).

<sup>b</sup>Reference 16.

<sup>c</sup>Reference 14.

<sup>d</sup>Reference 19.

<sup>e</sup>Reference 21.

<sup>f</sup>Reference 18.

<sup>g</sup>Reference 20.

<sup>h</sup>Reference 24.

<sup>i</sup>Reference 25.

determinations for Pt,<sup>18</sup> Ni,<sup>19</sup> Ag,<sup>18</sup> and Al,<sup>20</sup> is excellent. Experimental divacancy binding energies for Au,<sup>21</sup> and Cu,<sup>20</sup> are several tenths of an eV lower than the calculated values. The activation energy for divacancy migration  $E_{2V}^M$  is calculated to be slightly lower than that for monovacancy migration. Calculated values are in excellent agreement with the experimental measurements<sup>18</sup> for Au, Ag, Pt, Cu, and Al. The experimental divacancy migration energy for Ni is lower than the calculated value.<sup>19</sup>

A number of helium point-defect calculations have been performed to compare with experiment and previous calculations. Formation energies for interstitial ( $O_h$  site) helium  $E_{He}^F$  are found to range from 4.02 eV in Ni to 1.32 eV in Al and Ag. Previous calculations with a short-range potential give values of 4.02 eV in Ni,<sup>13</sup> and 1.97 eV in Cu,<sup>2</sup> in excellent agreement with the long-range potential. The higher formation energy in nickel is due to the inclusion of electronic effects in the He-Ni pair potential. Including these effects for the other metals would raise the calculated helium interstitial formation energy by ~1–2 eV. Migration energies  $E_{He}^M$  show a wide range from 1.13 eV for Pt to 0.33 eV for Al. The current values for Cu and Ni are in good agreement ( $\leq 0.2$  eV higher) with those previously calculated with a short-range metal-metal potential.<sup>2,13</sup> It has been shown<sup>13</sup> that the inclusion of quantum-mechanical effects (rather than using a free-electron helium-metal interaction) and the extrapolation to an infinite lat-

tice can lower the calculated helium migration energy in nickel by ~0.2 eV. The He-Ni pair potential used here compensates for more than half of this lowering. Thus the present Ni-Ni pair potential would predict a ~0.6 eV activation energy compared to ~0.4 eV using the Johnson Ni-Ni potential.<sup>13</sup> Similarly the helium migration energies for the other metals shown in Table III could be overestimates of the actual values by as much as 0.2 eV. It is found that the migration path for helium motion is along  $\langle 110 \rangle$  direction for all fcc metals considered except Ag where a  $\langle 111 \rangle$  path is found. No apparent reason for this path change is evident but it should be noted that for Ag the  $\langle 111 \rangle$  and  $\langle 110 \rangle$  paths are within 0.02 eV in migration energy. Binding energies for helium to a vacancy  $E_{HeV}^B$  are found to be quite large for all the metals considered, in good agreement with previous calculations for Cu,<sup>22</sup> and Ni,<sup>23</sup> and also with experimental measurements for Ni of ~2.1 eV,<sup>24</sup> and ~1 eV for Al.<sup>25</sup> This excellent agreement for Ni and Al with significantly different binding energies gives an important indication that point-defect properties can be accurately predicted by using the pair potentials developed here.

## V. CONCLUSIONS

A set of long-range pair potentials for various fcc metals has been derived. These potentials are fit to

many pieces of experimental data including the stacking-fault energy and sublimation energy. Two volume-dependent terms have been included in order to fit the experimental data. By using appropriate scaling factors a striking similarity between the various potentials is found. Various point-defect properties have been calculated, yielding good agreement with available experimental data.

#### ACKNOWLEDGMENTS

We would like to thank J. H. Holbrook of this laboratory for allowing us the use of his elasticity calculations and C. L. Bisson of this laboratory for providing the free-electron calculations. In addition we appreciate the fruitful discussions with W. D. Wilson, also of this laboratory. This work was supported by the Division of Basic Energy Sciences of the DOE.

#### APPENDIX A

By regrouping the terms in Eq. (3), an alternate expression may be obtained for the volume-dependent energy term

$$E_v = \Omega_0 \left( \frac{V}{V_0} \right) \sum_q \frac{p_q}{q!} \left( \frac{\Delta V}{V_0} \right)^q, \quad (\text{A1})$$

where  $\Delta V = V - V_0$  is the volume change and the  $p_q$  are constants that are easily related to the  $P_q$  of Eq. (3).

In using Eq. (A1) for the case of point defects, e.g., a vacancy, the definition of the undeformed volume  $V_0$  is ambiguous. For example, consider a perfect lattice of  $\sim 10^{23}$  atoms. Starting with  $N_A$

atoms and  $N_L = N_A$  lattice sites one can create a vacancy by moving an atom from the bulk to the surface thereby increasing the number of lattice sites by one keeping the number of atoms fixed. For  $N_A$  atoms,  $V_0 = N_A \Omega_0$ ,  $V = (N_A + 1) \Omega_0$ , and the volume contribution to the total energy is given by

$$N_A \Omega_0 \left( \frac{N_A + 1}{N_A} \right) \sum_q \frac{p_q}{q!} \left( \frac{1}{N_A} \right)^q.$$

On the other hand, a vacancy may also be created by removing an atom to infinity from a perfect lattice of  $N_A + 1$  atoms ( $N_L = N_A + 1$ ), thereby reducing  $N_A$  by one keeping  $N_L$  fixed. In this case  $V_0 = (N_A + 1) \Omega_0$ ,  $V = N_A \Omega_0$ , and the volume contribution to the total energy is given by  $(N_A + 1) \Omega_0 p_0$ . Since the final system in both cases is the same, the two energy expressions must be equal, yielding

$$(N_A + 1) \Omega_0 \sum_q \frac{p_q}{q!} \left( \frac{1}{N_A} \right)^q = (N_A + 1) \Omega_0 p_0. \quad (\text{A2})$$

Since  $N_A$  is large ( $\sim 10^{23}$ ) terms of order  $1/N_A$  or greater ( $q \geq 2$ ) vanish. The  $q = 0$  terms cancel identically, requiring only  $p_1 = 0$  to satisfy Eq. (A2). Since terms for  $q > 2$  only appear in second order or higher elastic constants, they are not needed here and are set equal to zero. The resultant volume-dependent term is given in Eq. (4). The  $P_q$  are given by

$$P_1 = p_0 + \frac{1}{2} p_2, \quad P_2 = -p_2, \quad P_3 = \frac{1}{2} p_2. \quad (\text{A3})$$

#### APPENDIX B

Some controversy exists in the literature regarding the changes in the energy of point defect due to

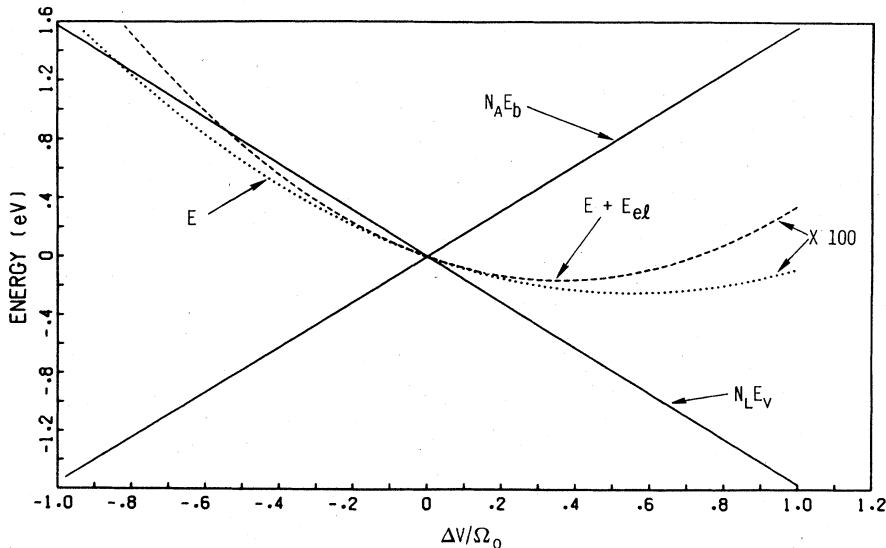


FIG. 4. Energy terms for a helium interstitial in nickel as a function of volume change. Note that the cancellation of the bond energy ( $N_A E_b$ ) and volume-dependent energy ( $N_L E_v$ ) terms necessitates a  $100 \times$  magnification of the atomistic energy curve ( $E = N_A E_b + N_L E_v$ ) as well as the total energy curve ( $E + E_{el}$ ) to show their details.

volume change.<sup>3,26,27</sup> This Appendix presents a detailed study of the effect of volume change on defect energy. For illustrative purposes the results of a single defect, i.e., a helium interstitial in nickel is presented here. A spherical region with 682 movable atoms was used. By varying the lattice constant, calculations of the total bond energy ( $N_A E_b$ ) as a function of volume change are obtained. These energies (relative to no volume change) are shown in Fig. 4. In addition the volume-dependent energy term ( $N_L E_v$ ) is also shown. Note that the large volume dependence of these two terms is nearly opposite and tend to cancel out near the lattice equilibrium. The total atomistic energy  $E = N_A E_b + N_L E_v$  (Fig. 4) shows a very shallow minimum (only 0.0025 eV below the energy for no volume change) at a lattice expansion of 0.55 atomic volumes.

To obtain the energy lowering and volume expansion in an infinite medium an additional elastic energy term must be added. This term represents the energy needed to compress the atomistic cluster used above to its undeformed state, insert it in a hole in an infinite medium, and then allow equilibrium. The elastic energy  $E_{el}$  required for these processes (as-

suming isotropic linear elasticity) is given by<sup>28</sup>

$$E_{el} = \frac{2\mu(\Delta V/\Omega_0)^2 \Omega_0}{3N(1+4\mu/3B^*)}, \quad (B1)$$

where  $\mu$  is the shear modulus of the infinite medium,  $B^*$  is the bulk modulus of the atomistic cluster, and  $N$  is the number of lattice atoms in the cluster. Using a shear modulus of 0.779 eV/Å<sup>3</sup> and a bulk modulus of 1.127 eV/Å<sup>3</sup> (consistent with the Ni elastic constants), the elastic energy is added to the atomistic energy. The resultant energy (also shown in Fig. 4) has a minimum of 0.0016 eV below the undeformed lattice and a volume expansion of 0.36 atomic volumes. Therefore it is seen that a fixed volume calculation for clusters of this size are able to give energies accurate to ~0.002 eV with respect to volume changes. Thus, it is not necessary and, in fact, is incorrect to modify defect energies by the volume-dependent energy (0.1–1.0 eV) as in Ref. 3 since this term is nearly canceled by the bond energy, the difference being <0.01 eV. Application of this incorrect "correction"<sup>3</sup> leads to the prediction of the crowdion rather than the <100> split interstitial as the stable interstitial configuration in nickel.

<sup>1</sup>R. A. Johnson, J. Phys. F **3**, 295 (1973).

<sup>2</sup>W. D. Wilson and C. L. Bisson, Phys. Rev. B **3**, 3984 (1971).

<sup>3</sup>K. M. Miller and P. D. Bristowe, Phys. Status Solidi B **86**, 93 (1978).

<sup>4</sup>R. A. Johnson, Phys. Rev. **145**, 423 (1966).

<sup>5</sup>A. Englert, H. Tompa, and R. Bullough, *Fundamental Aspects of Dislocation Theory* (National Bureau of Standards, Washington, 1970), Vol. 1, p. 273.

<sup>6</sup>K. Fuchs, Proc. R. Soc. London Sect. A **153**, 622 (1936); **157**, 444 (1936).

<sup>7</sup>R. A. Johnson, Phys. Rev. B **6**, 2094 (1972).

<sup>8</sup>C. S. Barrett and T. B. Massalski, *Structure of Metals* (McGraw-Hill, New York, 1966).

<sup>9</sup>G. Simmons and H. Wang, *Single Crystal Elastic Constants and Calculated Aggregate Properties; A Handbook* (MIT, Cambridge, Mass., 1971).

<sup>10</sup>*Metal Reference Book*, edited by C. J. Smith, 5th ed. (Butterworths, London, 1976), p. 186.

<sup>11</sup>*Vacancies and Interstitials in Metals*, edited by A. Seeger, D. Schumacher, W. Schilling, and J. Diehl (North-Holland, Amsterdam, 1970).

<sup>12</sup>J. P. Hirth and J. Lothe, *Theory of Dislocations* (McGraw-Hill, New York, 1968); C. B. Carter and S. M. Holmes, Philos. Mag. **35**, 1161 (1977); L. E. Murr, Scr. Metall. **6**, 203 (1972); N. I. Noskova and V. A. Pavlov, Fiz.

Metal. Metalloved. **20**, 428 (1965).

<sup>13</sup>C. F. Melius, C. L. Bisson, and W. D. Wilson, Phys. Rev. B **18**, 1647 (1978).

<sup>14</sup>F. W. Young, J. Nucl. Mater. **69-70**, 310 (1978).

<sup>15</sup>P. Ehrhart and U. Schlagheck, J. Phys. F **4**, 1575 (1974).

<sup>16</sup>V. Spirić, L. E. Rehn, K.-H. Robrock, and W. Schilling, Phys. Rev. B **15**, 672 (1977).

<sup>17</sup>J. R. Hardy, J. Phys. Chem. Solids **29**, 2009 (1968).

<sup>18</sup>J. S. Koehler, in *Vacancies and Interstitials in Metals*, edited by A. Seeger, D. Schumacher, W. Schilling, and J. Diehl (North-Holland, Amsterdam, 1970), p. 169.

<sup>19</sup>H. Kronmüller, in Ref. 18, p. 183.

<sup>20</sup>A. Seeger and H. Mehrer, in Ref. 18, p. 1.

<sup>21</sup>K. P. Chik, in Ref. 18, p. 183.

<sup>22</sup>W. D. Wilson, M. I. Baskes, and C. L. Bisson, Phys. Rev. B **13**, 2470 (1976).

<sup>23</sup>M. I. Baskes, C. L. Bisson, and W. D. Wilson, J. Nucl. Mater. (to be published).

<sup>24</sup>D. Edwards, Jr. and E. V. Kornelsen, Surf. Sci. **44**, 1 (1974). C. L. Snead, Jr., A. N. Goland, and F. W. Wiffen, J. Nucl. Mater. **64**, 195 (1977).

<sup>25</sup>J. P. Hirth, in *Interatomic Potentials and Simulation of Lattice Defects*, edited by P. C. Gehlen, J. R. Beeler, and R. I. Jaffee (Plenum, New York, 1972), p. 456.

<sup>26</sup>M. S. Duesbery, in Ref. 27, p. 458.

<sup>27</sup>H. Holbrook (private communication).